Mitigating Face Recognition Bias via Group Adaptive Classifier

Sixue Gong   **Xiaoming Liu**   **Anil K. Jain**
Michigan State University, East Lansing MI 48824
{gongsixu, liuxm, jain}@msu.edu

Abstract

Face recognition is known to exhibit bias - subjects in certain demographic group can be better recognized than other groups. This work aims to learn a fair face representation, where faces of every group could be equally well-represented. Our proposed group adaptive classifier, GAC, learns to mitigate bias by using adaptive convolution kernels and attention mechanisms on faces based on their demographic attributes. The adaptive module comprises kernel masks and channel-wise attention maps for each demographic group so as to activate different facial regions for identification, leading to more discriminative features pertinent to their demographics. We also introduce an automated adaptation strategy which determines whether to apply adaptation to a certain layer by iteratively computing the dissimilarity among demographic-adaptive parameters, thereby increasing the efficiency of the adaptation learning. Experiments on benchmark face datasets (RFW, LFW, IJB-A, and IJB-C) show that our framework is able to mitigate face recognition bias on various demographic groups as well as maintain the competitive performance.

1 Introduction

Face recognition (FR) systems are known to exhibit discriminatory behaviors against certain demographic groups [27, 37, 20]. The 2019 NIST Face Recognition Vendor Test [20] shows that all 106 FR algorithms that participated in the test exhibit varying biased performances on gender, race, and age groups of a mugshot dataset. Deploying biased FR systems for law enforcement is potentially unethical [11]. Given the importance of automated FR-driven decisions, it is crucial to develop fair and unbiased FR systems to avoid the negative societal impact. Note that we define FR bias as the uneven recognition performance with respect to demographic groups, which differs from the inductive bias in machine learning [14].

State-of-the-art (SOTA) FR algorithms [45, 65, 12] rely on convolutional neural networks (CNNs) trained on large-scale face datasets. The public training datasets for FR, *e.g.*, CASIA-WebFace [74], VGGFace2 [5], and MS-Celeb-1M [22], are collected by scraping face images off the web, with inevitable demographic bias [66]. Biases in data are transmitted to the FR models through network learning. For example, to minimize the overall loss, a network tends to learn a better representation for faces in the majority group whose number of faces dominate the training set, resulting in unequal discriminabilities. The imbalanced distribution of demographics in face data is, nevertheless, not the only trigger of FR bias. Prior works have shown that even using a demographic balanced dataset [66] or training separate classifiers for each group [37], the performance on some groups is still inferior to the others. By studying non-trainable FR algorithms, [37] introduced the notion of *inherent bias*, *i.e.*, certain groups are inherently more susceptible to errors in the face matching process.

To tackle the dataset-induced bias, traditional methods re-weight either the data proportions [6] or cost values [1]. Such methods are limited when applied to large-scale imbalanced datasets. Recent imbalance learning methods focus on novel objective functions for class-skewed datasets. For
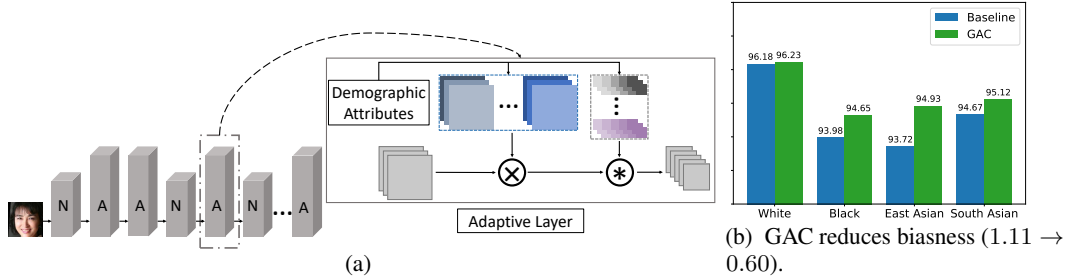
(a)

(b) GAC reduces biasness (1.11 → 0.60).

Figure 1: (a) Our proposed group adaptive classifier (GAC) automatically chooses between non-adaptive ("N") and adaptive ("A") layer in a multi-layer network, where the latter uses demographic-group-specific kernel and attention. (b) Compared to the baseline with the 50-layer ArcFace backbone, GAC improves face verification accuracy in most groups of RFW dataset [67], especially under-represented groups, leading to mitigated FR bias.

instance, Dong *et al*. [17] propose a Class Rectification Loss to incrementally optimize on hard samples of the classes with under-represented attributes. Alternatively, researchers strengthen the decision boundary to impede perturbation from other classes by enforcing margins between hard clusters via adaptive clustering [30], or between rare classes via Bayesian uncertainty estimates [35]. To adapt the aforementioned methods to racial bias mitigation, Wang *et al*. [66] modify the large margin based loss functions by reinforcement learning. However, [66] requires two auxiliary networks, an offline sampling network and a deep Q-learning network, to generate adaptive margin policy for training the FR network, which hinders the learning efficiency.

To mitigate FR bias, our main idea is to optimize the face representation learning on every demographic group in a single network, despite demographically imbalanced training data. Conceptually, we may categorize face features into two types of patterns: *general pattern* is shared by all faces; *differential pattern* is relevant to demographic attributes. When the differential pattern of one specific demographic group dominates training data, the network learns to predict identities mainly based on that pattern as it is more convenient to minimize the loss than using other patterns, thus bringing it bias towards faces of that specific group. One mitigation is to give the network more capacity to broaden its scope for multiple face patterns from different demographic groups. An unbiased FR model shall rely on not only unique patterns for recognition of different groups, but also general patterns of all faces for improved generalizability. Accordingly, as in Fig. 1, we propose a *group adaptive classifier* (GAC) to explicitly learn these different feature patterns. GAC includes two modules: the adaptive layer and automation module. The adaptive layer in GAC comprises adaptive convolution kernels and channel-wise attention maps where each kernel and attention map tackle faces in *one* demographic group.

Prior work on dynamic CNNs introduce adaptive convolutions to either every layer [33, 73, 68], or manually specified layers [47, 26, 63]. In contrast, this work proposes an automation module to choose which layers to apply adaptations. As we observed, not all convolutional layers require adaptive kernels for bias mitigation (see Fig. 4a). At any layer of GAC, only kernels expressing high dissimilarity are considered as demographic-adaptive kernels. For those with low dissimilarity, their average kernel is shared by all input images in that layer. Thus, the proposed network progressively learns to select the optimal structure for the demographic-adaptive learning. This enables that both non-adaptive layers with shared kernels and adaptive layers are jointly learned in a unified network.

The contributions of the paper are summarised as: 1) A new face recognition algorithm that reduces demographic bias and increases robustness of representations for faces in every demographic group by adopting adaptive convolutions and attention techniques; 2) A new adaptation mechanism that automatically determines the layers to employ dynamic kernels and attention maps; 3) The proposed method achieves SOTA performance on a demographic-balanced dataset and three benchmarks.

2   Related Work

Fairness Learning and De-biasing Algorithms. A variety of fairness techniques are proposed to prevent machine learning models from utilizing statistical bias in training data, including adversarial training [2, 25, 69, 48], subgroup constraint optimization [34, 81, 70], data pre-processing (*e.g.*, weighted sampling [21], and data transformation [4]), and algorithm post-processing [36, 54]. Another promising approach learns a fair representation to preserve all discerning information about the data

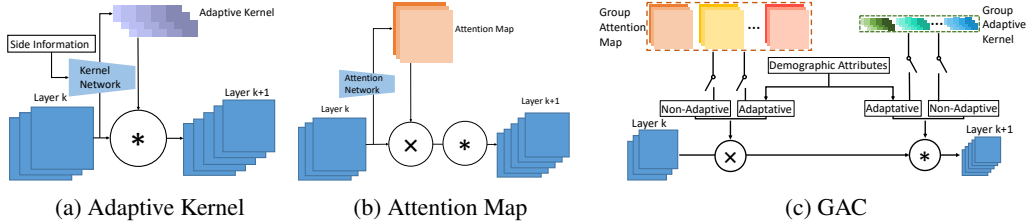|		
(a) Adaptive Kernel	(b) Attention Map	(c) GAC

Figure 2: A comparison of approaches in adaptive CNNs.

attributes or task-related attributes but eliminate the prejudicial effects from sensitive factors [51, 61, 77, 11, 23]. Locatello *et al.* [46] show the feature disentanglement is consistently correlated with increasing fairness of general purpose representations by analyzing $12,600$ SOTA models. Accordingly, a disentangled representation is learned to de-bias both FR and demographic attribute estimation [19]. Other studies address the bias issue in FR by leveraging unlabeled faces to improve the performance in groups with fewer samples [55, 67]. Wang *et al.* [66] propose skewness-aware reinforcement learning to mitigate racial bias in FR. Unlike prior work, our GAC is designed to customize the classifier for each demographic group, which, if successful, would lead to mitigated bias.

Adaptive Neural Networks. Three types of CNN-based adaptive learning techniques are related to our work: adaptive architectures, adaptive kernels, and attention mechanism. Adaptive architectures design new performance-based neural functions or structures, *e.g.*, neuron selection hidden layers [29] and automatic CNN expansion for FR [79]. As CNN advances many AI fields, prior works propose dynamic kernels to realize content-adaptive convolutions. Li *et al.* [40] propose a shape-driven kernel for facial trait recognition where each landmark-centered patch has a unique kernel. A convolution fusion for graph neural networks is introduced by [18] where a set of varying-size filters are used per layer. The works of [16] and [41] use a kernel selection scheme to automatically adjust the receptive field size based on inputs. To better suit input data, [15] splits training data into clusters and learns an exclusive kernel per cluster. Li *et al.* [42] introduce an adaptive CNN for object detection that transfers pre-trained CNNs to a target domain by selecting useful kernels per layer. Alternatively, one may feed input images or features into a kernel function to dynamically generate convolution kernels [62, 76, 39, 32]. Despite its effectiveness, such individual adaptation may not be suitable given the diversity of faces in demographic groups. Our work is most related to the side information adaptive convolution [33], where in each layer a sub-network inputs auxiliary information to generate filter weights. We mainly differ in that GAC automatically learns where to use adaptive kernels in a multi-layer CNN (see Figs. 2a and 2c), thus more efficient and capable in applying to a deeper CNN.

As the human perception process naturally selects the most pertinent piece of information, attention mechanisms are designed for a variety of tasks, *e.g.*, detection [78], recognition [9], image captioning [8], tracking [7], pose estimation [63], and segmentation [47]. Typically, attention weights are estimated by feeding images or feature maps into a shared network, composed of convolutional and pooling layers [3, 9, 43, 60] or multi-layer perceptron (MLP) [28, 71, 57, 44]. Apart from feature-based attention, Hou *et al.* [26] propose a correlation-guided cross attention map for few-shot classification where the correlation between the class feature and query feature generates the attention weights. The work of [73] introduces a cross-channel communication block to encourage information exchange across channels at the convolutional layer. To accelerate the channel interaction, Wang *et al.* [68] propose a 1D convolution across channels for attention prediction. Different from prior work, our attention maps are constructed by demographic information (see Figs. 2b and Fig. 2c), which improves the robustness of face representations in every demographic group.

3 Methodology

3.1 Overall Idea

Our goal is to train a FR network that is impartial to individuals in different demographic groups. Unlike image-related variations where face images with large poses or lower resolution are harder to be recognized, demographic attributes are subject-related properties with no apparent impact in recognizability of identity, at least from a layman's perspective. Thus, an unbiased FR system should be able to obtain equally salient features for faces across all demographic groups. However, due to imbalanced demographic distributions and inherent face differences between groups, it has been shown that higher performance is achieved on certain groups even with hand-crafted features [37].
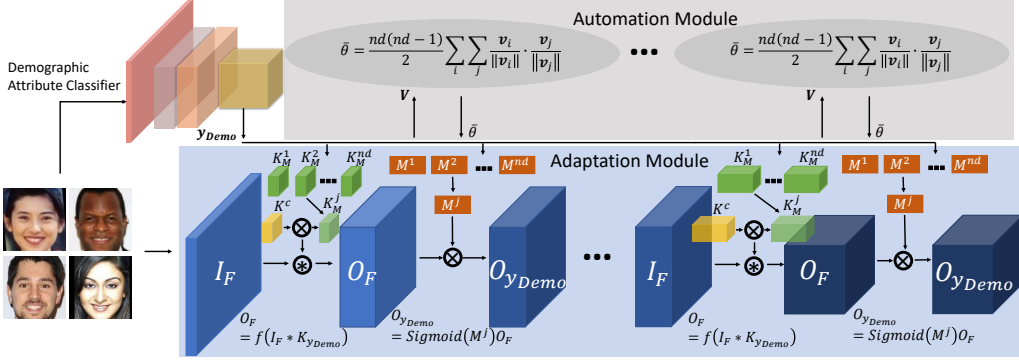
Figure 3: Overview of the proposed GAC for mitigating FR bias. GAC contains two major modules, *i.e.*, the adaptive layer and the automation module. The adaptive layer consists of adaptive kernels and attention maps. The automation module is employed to decide whether a layer should be adaptive or not.

Hence, it is impractical to extract features from different demographic groups that exhibit equal discriminability. Despite such disparity, a FR algorithm can still be designed to *mitigate* the difference in performance. To this end, we propose a CNN-based group adaptive classifier to utilize dynamic kernels and attention maps to boost FR performance in all demographic groups considered here. In particular, GAC has two main modules, an adaptive layer and an automation module. In adaptive layer, face images or feature maps are convolved with a unique kernel for each demographic group, and multiplied with adaptive attention maps to obtain demographic-differential features for faces in a certain group. The automation module determines in which layers of the network adaptive kernels and attention maps should be applied. Fig. 3 illustrates the overview of GAC. Given an aligned face image, and its identity label y_{ID}, a pre-trained demographic classifier first estimates its demographic attribute y_{Demo}. With y_{Demo}, the image is then fed into a recognition network with multiple demographic adaptive layers to estimate the identity of the input. In the following, we present these two modules.

3.2 Adaptive Layer

Adaptive Convolution. For a standard convolution operation in CNN, an image or feature map from the previous layer $I_F \in \mathbb{R}^{ic \times ih \times iw}$ is convolved with a single kernel matrix $K \in \mathbb{R}^{kc \times ic \times kh \times kw}$, where ic is the number of input channels, kc the number of filters, ih and iw the input size, and kh and kw the filter size. Such an operation shares the kernel with every input that goes through the layer, and is thus agnostic to demographic content, resulting in limited capacity to represent faces of groups with fewer samples. To mitigate the bias in convolution, we introduce a trainable matrix of kernel masks $K_M \in \mathbb{R}^{nd \times ic \times kh \times kw}$, where nd is the number of demographic groups. During the forward pass, the demographic label y_{Demo} and the kernel matrix K_M are fed to the adaptive convolutional layer to generate demographic adaptive filters. Let $K^c \in \mathbb{R}^{ic \times kh \times kw}$ denote the cth channel filter, and the adaptive filter weights for c^{th} channel are:

$$K^c_{y_{Demo}} = K^c \bigotimes K^j_M, \tag{1}$$

where $K^j_M \in \mathbb{R}^{ic \times kh \times kw}$ is the jth kernel mask for group y_{Demo}, and $\bigotimes$ denotes element-wise multiplication. Then the cth channel of the output feature map is given by $O^c_F = f(I_F * K^c_{y_{Demo}})$, where * denotes convolution, and $f(\cdot)$ is the activation function. In contrast to the conventional convolution, samples in every demographic group have a unique kernel $K_{y_{Demo}}$.

Adaptive Attention. Each channel filter in a CNN plays an important role in every dimension of the final representation, which can be viewed as a semantic pattern detector [8]. In the adaptive convolution, however, the values of a kernel mask are broadcast along the channel dimension, indicating that the weight selection is spatially varied but channel-wise joint. Hence, we introduce a channel-wise attention mechanism to enhance the face features that are demographic-adaptive. First, a trainable matrix of channel attention maps $M \in \mathbb{R}^{nd \times kc}$ is initialized in every adaptive attention layer. Given y_{Demo} and the current feature map $O_F \in \mathbb{R}^{kc \times oh \times ow}$, where oh and ow are the height and width of O_F, the cth channel of the new feature map is calculated by:

$$O^c_{y_{Demo}} = \text{Sigmoid}(M^{jc}) \cdot O^c_F, \tag{2}$$

where M^{jc} is the entry in the jth row of M for the demographic group y_{Demo} at c^{th} column. In contrast to the adaptive convolution, elements of each demographic attention map M^j diverge in channel-wise manner, while the single attention weight M^{jc} is spatially shared by the entire matrix $O_F^c \in \mathbb{R}^{oh \times ow}$. The two adaptive matrices, K_M and M, are jointly tuned with all the other parameters supervised by the classification loss.

Unlike dynamic CNNs [33] where additional networks are engaged to produce input-variant kernel or attention map, our adaptiveness is yielded by a simple thresholding function directly pointing to the demographic group with no auxiliary networks. Although the kernel network in [33] can generate continuous kernels without enlarging the parameter space, further encoding is required if the side inputs for kernel network are discrete variables. Our approach, in contrast, divides kernels into clusters so that the branch parameter learning can stick to a specific group without interference from individual uncertainties, making it suitable for discrete domain adaptation. Further, the adaptive kernel masks in GAC are more efficient in terms of the number of additional parameters. Compared to a non-adaptive layer, the number of additional parameters of GAC is $nd \times ic \times kh \times kw$, while that of [33] is $id \times kc \times ic \times kh \times kw$ if the kernel network is a one-layer MLP, where id is the dimension of input side information. Thus, for one adaptive layer, [33] has $\frac{id \times kc}{nd}$ times more parameters than ours, which can be substantial given the typical large value of kc, the number of filters.

3.3   Automation Module

Though faces in different demographic groups are adaptively processed by various kernels and attention maps, it is inefficient to use such adaptations in *every* layer of a deep CNN. To relieve the burden of unnecessary parameters and avoid empirical trimming, we adopt a similarity fusion process to automatically determine the adaptive layers. Since the same fusion scheme can be used for both types of adaptation, we take the adaptive convolution as an example to illustrate this automatic scheme. First, a matrix composed of nd kernel masks is initialized in every convolutional layer. As the training continues, each kernel mask is updated independently to reduce face classification loss for each demographic group. Second, we reshape the kernel masks into 1D vectors $\mathbf{V} = [\mathbf{v}_1, \mathbf{v}_2, \ldots, \mathbf{v}_{nd}]$, where $\mathbf{v}_i \in \mathbb{R}^l, l = ic \times kw \times kh$ represents the kernel mask of the ith demographic group. Next, we compute Cosine similarity between two kernel vectors, $\theta_{ij} = \frac{\mathbf{v}_i}{\|\mathbf{v}_i\|} \cdot \frac{\mathbf{v}_j}{\|\mathbf{v}_j\|}$, where $i, j \in \{1, 2, \ldots, nd\}$.

The average similarity of all pair-wise Cosine values is obtained by $\bar{\theta} = \frac{nd(nd-1)}{2} \sum_i \sum_j \theta_{ij}, i \neq j$.

If $\bar{\theta}$ is higher than a pre-defined threshold τ, the kernel parameters in this layer reveal the demographic-agnostic property. Hence, we merge the nd kernels into a single kernel by taking the average along the group dimension. In the subsequent training, this single kernel can still be updated separately for each demographic group, since the kernels may become demographic-adaptive in later epochs. We monitor the similarity trend of the adaptive kernels in each layer until $\bar{\theta}$ is stable.

4   Experiments

Datasets: Our bias study uses RFW dataset [67] for testing and BUPT-Balancedface dataset [66] for training. RFW consists of faces in four race/ethnic groups: White, Black, East Asian, and South Asian [1]. Each group contains $\sim$10K images of 3K individuals for face verification. BUPT-Balancedface contains 1.3M images of 28K celebrities and is approximately race-balanced with 7K identities per race. Other than race, we also consider gender bias in face representation learning. We combine IMDB [56], UTKFace [80], AgeDB [50], AAF [10], AFAD [52] to train a gender classifier, which is used to estimate gender of faces on RFW and BUPT-Balancedface. All face images are cropped and resized to 112×112 pixels via landmarks detected by RetinaFace [13].

Implementation Details: We train a baseline network and GAC on BUPT-Balancedface, using the 50-layer ArcFace architecture [12]. The classification loss is an additive Cosine margin in Cosface [65], with the scale and margin of $s = 64$ and $m = 0.5$. Training is optimized by SGD with a momentum of 0.9, a weight decay 0.01 and a batch size 256. The learning rate starts from 0.1 and drops to 0.0001 following the schedule at 8, 13, 15 epochs for the baseline, and 5, 17, 19 epochs for GAC. $\tau = 0$ is chosen for automatic adaptation in GAC. Our FR models are trained to extract a 512-dim representation. Our demographic classifier uses a 18-layer ResNet [24]. Comparing the GAC and baseline, the average feature extraction speed per image on Nvidia 1080Ti GPU is 1.4ms and 1.1ms, and the number of model parameters is 44.0M and 43.6M, respectively.

---

[1] RFW [67] uses Caucasian, African, Asian, and Indian to name demographic groups. We adopt these groups and accordingly rename to White, Black, East Asian, and South Asian for clearer race/ethnicity definition.

	Method	White	Black	East Asian	South Asian	Avg	STD
SOTA	RL-RBN [66]	96.27	95.00	94.82	94.68	95.19	0.63
	ACNN [33]	96.12	94.00	93.67	94.55	94.58	0.94
	PFE [59]	96.38	**95.17**	94.27	94.60	95.11	0.93
Ablation	Baseline	96.18	93.98	93.72	94.67	94.64	1.11
	GAC-Channel	95.95	93.67	94.33	94.78	94.68	0.83
	GAC-Kernel	96.23	94.40	94.27	94.80	94.93	0.78
	GAC-Spatial	95.97	93.20	93.67	93.93	94.19	1.06
	GAC-CS	96.22	93.95	94.32	95.12	94.65	0.87
	GAC-CSK	96.18	93.58	94.28	94.83	94.72	0.95
	GAC-($\tau = -0.1$)	**96.52**	94.35	94.63	94.77	95.07	0.85
	GAC-($\tau = 0.1$)	96.25	93.95	93.82	94.77	94.70	0.97
	GAC	96.23	94.65	**94.93**	**95.12**	**95.23**	**0.60**

Table 1: Verification Accuracy (%) on the protocol of RFW [67].

Method	Gender	White	Black	East Asian	South Asian	Avg	STD
Baseline	Male	97.49 ± 0.08	96.94 ± 0.26	97.29 ± 0.09	97.03 ± 0.13	96.96 ± 0.03	0.69 ± 0.04
	Female	97.19 ± 0.10	97.93 ± 0.11	95.71 ± 0.11	96.01 ± 0.08		
AL+Manual	Male	98.57 ± 0.10	98.05 ± 0.17	98.50 ± 0.12	$\mathbf{98.36 \pm 0.02}$	98.09 ± 0.05	0.66 ± 0.07
	Female	98.12 ± 0.18	$\mathbf{98.97 \pm 0.13}$	96.83 ± 0.19	97.33 ± 0.13		
GAC	Male	$\mathbf{98.75 \pm 0.04}$	98.18 ± 0.20	$\mathbf{98.55 \pm 0.07}$	98.31 ± 0.12	$\mathbf{98.19 \pm 0.06}$	$\mathbf{0.56 \pm 0.05}$
	Female	98.26 ± 0.16	98.80 ± 0.15	$\mathbf{97.09 \pm 0.12}$	$\mathbf{97.56 \pm 0.10}$		

Table 2: Verification Accuracy (%) of 5-fold cross-validation on 8 groups of RFW [67].

4.1 Results on RFW Protocol

We first follow RFW face verification protocol with 6K pairs per race/ethnicity. The models are trained on BUPT-Balancedface with ground truth race/ethnicity and identity labels. The common group fairness criteria like demographic parity distance are improper to evaluate fairness of learnt representations, since they are typically designed to measure independence properties of random variables. However, in FR the sensitive demographic characteristics are tied to identities, making these two variables correlated. The NIST report proposes to use false negative and false positive for each demographic group to measure the fairness [20]. Instead of plotting false negative vs. false positives, we use a compact quantitative measure, *i.e.*, the standard deviation (STD) of the performance in different demographic groups, that was previously introduced in [66, 19] and called "biasness". We also report average accuracy (Avg) to show the overall FR performance.

Ablation Deep feature maps contain both spatial and channel-wise information. Here we investigate the relationship among adaptive kernels, spatial and channel-wise attentions, and their impact to bias mitigation. We also study the impact of τ in our automation module. Apart from the baseline and GAC, we ablate seven variants: (1) GAC-Channel: channel-wise attention for race-differential feature; (2) GAC-Kernel: adaptive convolution with race-specific kernels; (3) GAC-Spatial: only spatial attention is added to baseline; (4) GAC-CS: both channel-wise and spatial attention; (5) GAC-CSK: combine adaptive convolution with spatial and channel-wise attention; (6,7) GAC-($\tau = *$): set τ to $*$.

Since the approach in ACNN [33] is related to GAC, we re-implement it and apply to the bias mitigation problem. First, we train a race classifier with the cross-entropy loss on BUPT-Balancedface. Then the softmax output of our race classifier is fed to a filter manifold network (FMN) to generate adaptive filter weights. Here, FMN is a two-layer MLP with a ReLU in between. Similar to GAC, race probabilities are considered as auxiliary information for face representation learning. We also compare with the SOTA approach PFE [59] via training a PFE model on BUPT-Balancedface.

Tab. 1 reports the results of SOTA algorithms and ablation variants on RFW protocol. We make several observations: (1) the baseline model is the most biased across race groups. (2) spatial attention mitigates the race bias at the cost of verification accuracy, and is less effective on learning fair features than other adaptive techniques. This is probably because spatial contents, especially local layout information, only reside at earlier CNN layers, where the spatial dimensions are gradually decreased by the following convolutions and poolings. Therefore, semantic details like demographic attributes are hardly encoded spatially. (3) Compared to GAC, combining adaptive kernels with both spatial and channel-wise attention increases the number of parameters, lowering the performance. (4) As τ determines the number of adaptive layers in GAC, it has a great impact on the performance. A small τ may increase redundant adaptive layers, while the adaptation layers may lack in capacity if too large. (5) GAC is superior to SOTA w.r.t. average performance and feature fairness. Compared to kernel masks in GAC, the FMN in ACNN [33] contains more trainable parameters. Applying it to each convolutional layer is prone to overfitting. In fact, eight layers are empirically chosen as the FMN based convolution. (6) Even though PFE performs the best on standard benchmarks (Tab. 3),
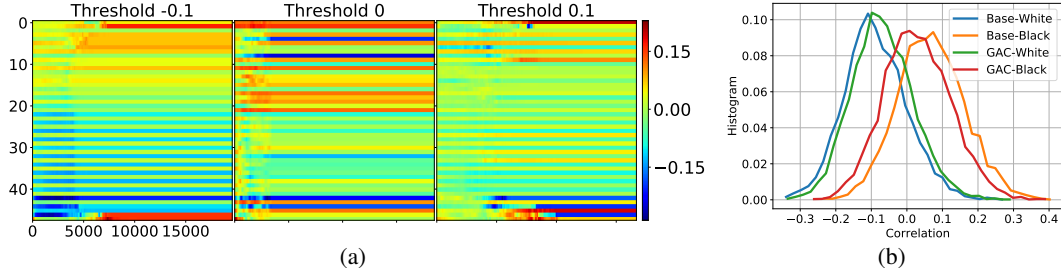
Figure 4: (a) For each of the three τ values in automatic adaptation, we show the average negative Cosine values of the pair-wise demographic kernel masks, *i.e.*, $\bar{\theta}$, at $1 - 48$ layers (y-axis), and $1 - 20K$ training steps (x-axis). The number of adaptive layers in the three cases, *i.e.*, $\sum_1^{48}(\bar{\theta} > \tau)$ at $20K^{th}$ step, are 39, 19, and 3, respectively. (b) With two race groups (White and Black in PCSO [37]) and two models (baseline and GAC), for each of the 4 combinations, we compute pair-wise correlation of face representations using any two out of $1K$ subjects in the same race, and plot the histogram of correlations. GAC reduces the difference/bias of two distributions.

Method	LFW (%)	Method	IJB-A (%) 0.1% FAR	IJB-C @ FAR (%) 0.001%	0.01%	0.1%
DeepFace+ [64]	97.35	Yin *et al.* [75]	73.9 ± 4.2	-	-	69.3
CosFace [65]	99.73	Cao *et al.* [5]	90.4 ± 1.4	74.7	84.0	91.0
ArcFace [12]	**99.83**	Multicolumn [72]	*92.0 ± 1.3*	<u>77.1</u>	<u>86.2</u>	<u>92.7</u>
PFE [59]	*99.82*	PFE [59]	$\mathbf{95.3 \pm 0.9}$	**89.6**	**93.3**	**95.5**
Baseline	99.38	Baseline	90.2 ± 1.1	80.2	88.0	92.9
GAC	<u>99.75</u>	GAC	<u>91.3 ± 1.2</u>	*83.5*	*89.2*	*93.7*

Table 3: Verification Performance on LFW, IJB-A, and IJB-C. [Key: **Best**, *Second*, <u>Third</u> Best]

it still exhibits high biasness. Our GAC outperforms PFE on RFW in both biasness and average performance. As the race data is a four-element input in our case, using extra kernel networks adds complexity to the FR network, which degrades the verification performance. Fig. 6 shows pairs of false positives (two faces falsely verified as the same identity) and false negatives (two faces falsely verified as different identities) produced by the baseline but successfully verified by GAC.

4.2   Results on Gender and Race Groups

We now extend demographic attributes to both gender and race. First, we train two classifiers that predict gender and race/ethnicity of a face image. The classification accuracy of gender and race/ethnicity is 85% and 81%[2], respectively. Then, these fixed classifiers are affiliated with GAC to provide demographic information for learning adaptive kernels and attention maps. We merge BUPT-Balancedface and RFW, and split the subjects into 5 sets for each of 8 demographic groups. In 5-fold cross-validation, each time a model is trained on 4 sets and tested on the remaining set.

Here we demonstrate the efficacy of the automation module for training the GAC. We compare to the scheme of manually design (AL+Manual) that adds adaptive kernels and attention maps to a subset of layers. Specifically, the first block in every residual unit is chosen to be the adaptive convolution layer, and channel-wise attentions are applied to the feature map output by the last block in every residual unit. As 4 residual units are in our network and each block has 2 convolutional layers, the manual scheme involves 8 adaptive convolutional layers and 4 groups of channel-wise attention maps. As shown in Tab. 2, automatic adaptation is more effective in enhancing the discriminability and fairness of face representations. Figure 4a shows the dissimilarity of kernel masks in the convolutional layers changes during training epochs under three threshold values τ. A lower τ results in more adaptive layers. We see the layers that are determined to be adaptive do vary across both layers (vertically) and training time (horizontally), which shows the importance of our automatic mechanism.

---

[2]This seemingly low accuracy is mainly due to the large dataset we assembled for training and testing gender/race classification. Our demographic classifier has been shown to perform comparably as SOTA on common benchmarks. While demographic estimation errors impact the training, testing, and evaluation of bias mitigation algorithms, the evaluation is of the most concern as errors in demographic labels may greatly impact the biasness calculation. Thus, future development may include either manually cleaning the labels, or designing a biasness metric robust to demographic label errors.

Race	Mean		STD		Relative Entropy	
	Baseline	GAC	Baseline	GAC	Baseline	GAC
White	1.15	1.17	0.30	0.31	0.0	0.0
Black	1.07	1.10	0.27	0.28	0.61	0.43
East Asian	1.08	1.10	0.31	0.32	0.65	0.58
South Asian	1.15	1.18	0.31	0.32	0.19	0.13

Table 4: Distribution of ratios between minimum inter-class distance and maximum intra-class distance of face features in 4 race groups of RFW. GAC exhibits higher ratios, and more similar distributions to the reference.

4.3 Results on Standard Benchmark Datasets

While our GAC mitigates bias, we also hope it can perform well on standard benchmarks. Therefore, we also evaluate GAC on standard benchmarks without considering demographic impacts, including LFW [31], IJB-A [38], and IJB-C [49]. These datasets exhibit imbalanced distribution in demographics. For a fair comparison with SOTA, instead of using ground truth demographics, we train GAC on Ms-Celeb-1M [22] with the demographic attributes estimated by the classifier pre-trained in Sec. 4.2. As in shown Tab. 3, GAC outperforms the baseline and achieves comparable performance to SOTA.
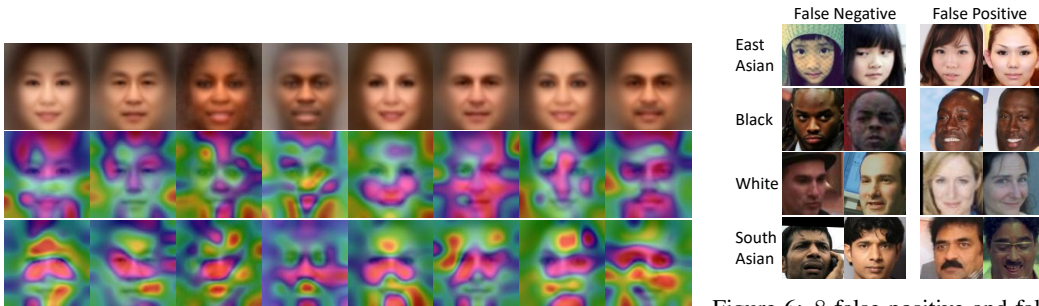

Figure 5: The first row shows the average faces of 8 groups in RFW. The next two rows show gradient-weighted class activation heatmaps [58] at the 43th convolutional layer of the GAC (Row 2) and baseline (Row 3).

Figure 6: 8 false positive and false negative pairs on RFW given by the baseline but successfully verified by GAC.

4.4 Visualization and Analysis on Bias of FR

Visualization: To understand the adaptive kernels in GAC, we visualize the feature maps at an adaptive layer for faces of various demographics, via a Pytorch visualization tool [53]. We visualize important regions of faces pertaining to the FR decision by using a gradient-weighted class activation mapping (Grad-CAM) [58]. Grad-CAM uses the gradients back from the final layer corresponding to an input identity, and guides the target feature map to highlight import regions for identity predicting. Figure 5 shows that, compared to the baseline model, the salient regions of GAC demonstrate more diversity on faces from different groups. This illustrates the variability of parameters in GAC for each group.

Bias via local geometry: In addition to STD, we also explain the bias phenomenon via the local geometry of a given face representation in each demographic group. We assume that the statistics of neighbors of a given point (representation) reflects certain properties of its manifold (local geometry). Accordingly, we first illustrate the pair-wise correlation of face representations. To minimize variations caused by other latent variables, we use constrained frontal faces of a mug shot dataset, PCSO [37], to show the demographic impact on the divergence of face features. We randomly select 1K White and 1K Black subjects from PCSO, and compute their pair-wise correlation within each race. In Fig. 4b, we discover that Base-White representations have lower inter-class correlation than Base-Black, *i.e.*, faces in the White group are over-represented by the baseline than Black. In contrast, GAC-White and GAC-Black shows more similarity in their correlation histograms.

Since PCSO has few Asian subjects, we use RFW to design a second way to examine the local geometry in four race groups. Specifically, after normalizing the representations, we compute the pair-wise Euclidean distance and measure the ratio between the minimum distance of inter-subjects pairs and the maximum distance of intra-subject pairs. We compute the mean and standard deviation (STD) of the ratio distributions in four groups, with two models. Also, we gauge the relative entropy to measure the deviation of the distributions from each other. For simplicity, we choose White group as the reference distribution. Tab. 4 shows that, while GAC has minor improvement over baseline in the mean, it gives smaller relative entropy in the other three groups, which indicates that the ratio

distributions of other races in GAC are more similar, *i.e.*, less biased, to the reference distribution. These results demonstrate the capability of GAC to increase fairness of face representations.

5   Conclusion

This paper tackles the issue of demographic bias in face recognition by learning a fair face representation. A group adaptive classifier (GAC) is proposed to improve robustness of representations for every demographic group considered here. Both adaptive convolution kernels and channel-wise attention maps are introduced to GAC. We further add an automatic adaptation module to determine whether to use adaptations in a given layer. Our findings suggest that faces can be better represented by using layers adaptive to different demographic groups, leading to more balanced performance gain for all groups. As GAC is agnostic to network architecture, one of our future directions is to apply GAC to various backbone networks, for both validation and further improving the face recognition performance.

Broader Impact

As face recognition (FR) systems are being deployed in the real world for societal benefit, it is desirable to develop an approach that is unbiased towards different demographic groups. De-biasing a FR algorithm while maintaining its average performance could be challenging due to the lack of discriminability in under-represented groups. Our approach addresses this problem via a group classifier mechanism that leverages both attention and adaptive learning strategies, which can be extended to other group fairness learning tasks as well.

References

[1] Rehan Akbani, Stephen Kwek, and Nathalie Japkowicz. Applying support vector machines to imbalanced datasets. In *ECML*. Springer, 2004.

[2] Mohsan Alvi, Andrew Zisserman, and Christoffer Nellåker. Turning a blind eye: Explicit removal of biases and variation from deep neural network embeddings. In *ECCV*, 2018.

[3] Alexei A Bastidas and Hanlin Tang. Channel attention networks. In *CVPR Workshops*, 2019.

[4] Flavio Calmon, Dennis Wei, Bhanukiran Vinzamuri, Karthikeyan Natesan Ramamurthy, and Kush R Varshney. Optimized pre-processing for discrimination prevention. In *NeurIPS*, 2017.

[5] Qiong Cao, Li Shen, Weidi Xie, Omkar M Parkhi, and Andrew Zisserman. VGGface2: A dataset for recognising faces across pose and age. In *FRGC*. IEEE, 2018.

[6] Nitesh V Chawla, Kevin W Bowyer, Lawrence O Hall, and W Philip Kegelmeyer. Smote: synthetic minority over-sampling technique. *Journal of Artificial Intelligence Research*, 2002.

[7] Boyu Chen, Peixia Li, Chong Sun, Dong Wang, Gang Yang, and Huchuan Lu. Multi attention module for visual tracking. *Pattern Recognition*, 2019.

[8] Long Chen, Hanwang Zhang, Jun Xiao, Liqiang Nie, Jian Shao, Wei Liu, and Tat-Seng Chua. SCA-CNN: Spatial and channel-wise attention in convolutional networks for image captioning. In *CVPR*, 2017.

[9] Zetao Chen, Lingqiao Liu, Inkyu Sa, Zongyuan Ge, and Margarita Chli. Learning context flexible attention model for long-term visual place recognition. *IEEE Robotics and Automation Letters*, 2018.

[10] Jingchun Cheng, Yali Li, Jilong Wang, Le Yu, and Shengjin Wang. Exploiting effective facial patches for robust gender recognition. *Tsinghua Science and Technology*, 24(3):333–345, 2019.

[11] Elliot Creager, David Madras, Joern-Henrik Jacobsen, Marissa Weis, Kevin Swersky, Toniann Pitassi, and Richard Zemel. Flexibly fair representation learning by disentanglement. In *ICML*, 2019.

[12] Jiankang Deng, Jia Guo, Niannan Xue, and Stefanos Zafeiriou. Arcface: Additive angular margin loss for deep face recognition. In *CVPR*, 2019.

[13] Jiankang Deng, Jia Guo, Zhou Yuxiang, Jinke Yu, Irene Kotsia, and Stefanos Zafeiriou. Retinaface: Single-stage dense face localisation in the wild. In *arxiv*, 2019.

[14] Thomas G Dietterich and Eun Bae Kong. Machine learning bias, statistical bias, and statistical variance of decision tree algorithms. Technical report, Department of Computer Science, Oregon State University, 1995.

[15] Chen Ding, Ying Li, Yong Xia, Wei Wei, Lei Zhang, and Yanning Zhang. Convolutional neural networks based hyperspectral image classification method with adaptive kernels. *Remote Sensing*, 2017.

[16] Chen Ding, Ying Li, Yong Xia, Lei Zhang, and Yanning Zhang. Automatic kernel size determination for deep neural networks based hyperspectral image classification. *Remote Sensing*, 2018.

[17] Qi Dong, Shaogang Gong, and Xiatian Zhu. Imbalanced deep learning by minority class incremental rectification. *IEEE Transactions on Pattern Analysis and Machine Intelligence*, 2018.

[18] Jian Du, Shanghang Zhang, Guanhang Wu, José MF Moura, and Soummya Kar. Topology adaptive graph convolutional networks. *arXiv preprint arXiv:1710.10370*, 2017.

[19] Sixue Gong, Xiaoming Liu, and Anil K Jain. Debface: De-biasing face recognition. *arXiv preprint arXiv:1911.08080*, 2019.

[20] Patrick Grother, Mei Ngan, and Kayee Hanaoka. Face recognition vendor test (FRVT) part 3: Demographic effects. In *Technical Report, National Institute of Standards and Technology*, 2019.

[21] Aditya Grover, Jiaming Song, Ashish Kapoor, Kenneth Tran, Alekh Agarwal, Eric J Horvitz, and Stefano Ermon. Bias correction of learned generative models using likelihood-free importance weighting. In *NeurIPS*, 2019.

[22] Yandong Guo, Lei Zhang, Yuxiao Hu, Xiaodong He, and Jianfeng Gao. Ms-celeb-1m: A dataset and benchmark for large-scale face recognition. In *ECCV*, 2016.

[23] Moritz Hardt, Eric Price, and Nati Srebro. Equality of opportunity in supervised learning. In *NeurIPS*, 2016.

[24] Kaiming He, Xiangyu Zhang, Shaoqing Ren, and Jian Sun. Deep residual learning for image recognition. In *CVPR*, 2016.

[25] Lisa Anne Hendricks, Kaylee Burns, Kate Saenko, Trevor Darrell, and Anna Rohrbach. Women also snowboard: Overcoming bias in captioning models. In *ECCV*, 2018.

[26] Ruibing Hou, Hong Chang, MA Bingpeng, Shiguang Shan, and Xilin Chen. Cross attention network for few-shot classification. In *NeurIPS*, 2019.

[27] J Howard, Y Sirotin, and A Vemury. The effect of broad and specific demographic homogeneity on the imposter distributions and false match rates in face recognition algorithm performance. In *IEEE BTAS*, 2019.

[28] Jie Hu, Li Shen, and Gang Sun. Squeeze-and-excitation networks. In *CVPR*, 2018.

[29] Ting-Kuei Hu, Yen-Yu Lin, and Pi-Cheng Hsiu. Learning adaptive hidden layers for mobile gesture recognition. In *AAAI*, 2018.

[30] Chen Huang, Yining Li, Change Loy Chen, and Xiaoou Tang. Deep imbalanced learning for face recognition and attribute prediction. *IEEE Transactions on Pattern Analysis and Machine Intelligence*, 2019.

[31] Gary B Huang, Marwan Mattar, Tamara Berg, and Eric Learned-Miller. Labeled faces in the wild: A database forstudying face recognition in unconstrained environments. 2008.

[32] Xu Jia, Bert De Brabandere, Tinne Tuytelaars, and Luc V Gool. Dynamic filter networks. In *NeurIPS*, 2016.

[33] Di Kang, Debarun Dhar, and Antoni Chan. Incorporating side information by adaptive convolution. In *NeurIPS*, 2017.

[34] Michael Kearns, Seth Neel, Aaron Roth, and Zhiwei Steven Wu. An empirical study of rich subgroup fairness for machine learning. In *Proceedings of the Conference on Fairness, Accountability, and Transparency*, 2019.

[35] Salman Khan, Munawar Hayat, Syed Waqas Zamir, Jianbing Shen, and Ling Shao. Striking the right balance with uncertainty. In *CVPR*, 2019.

[36] Michael P Kim, Amirata Ghorbani, and James Zou. Multiaccuracy: Black-box post-processing for fairness in classification. In *AAAI/ACM*, 2019.

[37] Brendan F Klare, Mark J Burge, Joshua C Klontz, Richard W Vorder Bruegge, and Anil K Jain. Face recognition performance: Role of demographic information. *IEEE Trans. Information Forensics and Security*, 7(6):1789–1801, 2012.

[38] Brendan F Klare, Ben Klein, Emma Taborsky, Austin Blanton, Jordan Cheney, Kristen Allen, Patrick Grother, Alan Mah, and Anil K Jain. Pushing the frontiers of unconstrained face detection and recognition: Iarpa janus benchmark a. In *CVPR*, 2015.

[39] Benjamin Klein, Lior Wolf, and Yehuda Afek. A dynamic convolutional layer for short range weather prediction. In *CVPR*, 2015.

[40] Shaoxin Li, Junliang Xing, Zhiheng Niu, Shiguang Shan, and Shuicheng Yan. Shape driven kernel adaptation in convolutional neural network for robust facial traits recognition. In *CVPR*, 2015.

[41] Xiang Li, Wenhai Wang, Xiaolin Hu, and Jian Yang. Selective kernel networks. In *CVPR*, 2019.

[42] Xudong Li, Mao Ye, Yiguang Liu, and Ce Zhu. Adaptive deep convolutional neural networks for scene-specific object detection. *IEEE Transactions on Circuits and Systems for Video Technology*, 2017.

[43] Hefei Ling, Jiyang Wu, Junrui Huang, Jiazhong Chen, and Ping Li. Attention-based convolutional neural network for deep face recognition. *Multimedia Tools and Applications*, 2020.

[44] Drew Linsley, D Schiebler, Sven Eberhardt, and Thomas Serre. Learning what and where to attend. In *ICLR*, 2019.

[45] Weiyang Liu, Yandong Wen, Zhiding Yu, Ming Li, Bhiksha Raj, and Le Song. Sphereface: Deep hypersphere embedding for face recognition. In *CVPR*, 2017.

[46] Francesco Locatello, Gabriele Abbati, Thomas Rainforth, Stefan Bauer, Bernhard Schölkopf, and Olivier Bachem. On the fairness of disentangled representations. In *NeurIPS*, 2019.

[47] Xiankai Lu, Wenguan Wang, Chao Ma, Jianbing Shen, Ling Shao, and Fatih Porikli. See more, know more: Unsupervised video object segmentation with co-attention siamese networks. In *CVPR*, 2019.

[48] David Madras, Elliot Creager, Toniann Pitassi, and Richard Zemel. Learning adversarially fair and transferable representations. In *ICML*, 2018.

[49] Brianna Maze, Jocelyn Adams, James A Duncan, Nathan Kalka, Tim Miller, Charles Otto, Anil K Jain, W Tyler Niggel, Janet Anderson, Jordan Cheney, et al. IARPA janus benchmark-c: Face dataset and protocol. In *2018 ICB*, 2018.

[50] Stylianos Moschoglou, Athanasios Papaioannou, Christos Sagonas, Jiankang Deng, Irene Kotsia, and Stefanos Zafeiriou. Agedb: the first manually collected, in-the-wild age database. In *CVPRW*, 2017.

[51] Daniel Moyer, Shuyang Gao, Rob Brekelmans, Aram Galstyan, and Greg Ver Steeg. Invariant representations without adversarial training. In *NeurIPS*, 2018.

[52] Zhenxing Niu, Mo Zhou, Le Wang, Xinbo Gao, and Gang Hua. Ordinal regression with multiple output cnn for age estimation. In *CVPR*, 2016.

[53] Utku Ozbulak. Pytorch cnn visualizations. `https://github.com/utkuozbulak/pytorch-cnn-visualizations`, 2019.

[54] Geoff Pleiss, Manish Raghavan, Felix Wu, Jon Kleinberg, and Kilian Q Weinberger. On fairness and calibration. In *NeurIPS*, 2017.

[55] Haoyu Qin. Asymmetric rejection loss for fairer face recognition. *arXiv preprint arXiv:2002.03276*, 2020.

[56] Rasmus Rothe, Radu Timofte, and Luc Van Gool. Deep expectation of real and apparent age from a single image without facial landmarks. *IJCV*, 2018.

[57] Muhammad Sadiq, Daming Shi, Meiqin Guo, and Xiaochun Cheng. Facial landmark detection via attention-adaptive deep network. *IEEE Access*, 2019.

[58] Ramprasaath R Selvaraju, Michael Cogswell, Abhishek Das, Ramakrishna Vedantam, Devi Parikh, and Dhruv Batra. Grad-cam: Visual explanations from deep networks via gradient-based localization. In *ICCV*, 2017.

[59] Yichun Shi and Anil K Jain. Probabilistic face embeddings. In *ICCV*, 2019.

[60] Vishwanath A Sindagi and Vishal M Patel. Ha-ccn: Hierarchical attention-based crowd counting network. *IEEE Transactions on Image Processing*, 2019.

[61] Jiaming Song, Pratyusha Kalluri, Aditya Grover, Shengjia Zhao, and Stefano Ermon. Learning controllable fair representations. In *ICAIS*, 2019.

[62] Hang Su, Varun Jampani, Deqing Sun, Orazio Gallo, Erik Learned-Miller, and Jan Kautz. Pixel-adaptive convolutional neural networks. In *CVPR*, 2019.

[63] Kai Su, Dongdong Yu, Zhenqi Xu, Xin Geng, and Changhu Wang. Multi-person pose estimation with enhanced channel-wise and spatial information. In *CVPR*, 2019.

[64] Yaniv Taigman, Ming Yang, Marc'Aurelio Ranzato, and Lior Wolf. Deepface: Closing the gap to human-level performance in face verification. In *CVPR*, 2014.

[65] Hao Wang, Yitong Wang, Zheng Zhou, Xing Ji, Dihong Gong, Jingchao Zhou, Zhifeng Li, and Wei Liu. Cosface: Large margin cosine loss for deep face recognition. In *CVPR*, 2018.

[66] Mei Wang and Weihong Deng. Mitigate bias in face recognition using skewness-aware reinforcement learning. *arXiv preprint arXiv:1911.10692*, 2019.

[67] Mei Wang, Weihong Deng, Jiani Hu, Xunqiang Tao, and Yaohai Huang. Racial faces in the wild: Reducing racial bias by information maximization adaptation network. In *ICCV*, 2019.

[68] Qilong Wang, Banggu Wu, Pengfei Zhu, Peihua Li, Wangmeng Zuo, and Qinghua Hu. Eca-net: Efficient channel attention for deep convolutional neural networks. *arXiv preprint arXiv:1910.03151*, 2019.

[69] Tianlu Wang, Jieyu Zhao, Mark Yatskar, Kai-Wei Chang, and Vicente Ordonez. Balanced datasets are not enough: Estimating and mitigating gender bias in deep image representations. In *CVPR*, 2019.

[70] Zeyu Wang, Klint Qinami, Yannis Karakozis, Kyle Genova, Prem Nair, Kenji Hata, and Olga Russakovsky. Towards fairness in visual recognition: Effective strategies for bias mitigation. *arXiv preprint arXiv:1911.11834*, 2019.

[71] Sanghyun Woo, Jongchan Park, Joon-Young Lee, and In So Kweon. Cbam: Convolutional block attention module. In *ECCV*, 2018.

[72] Weidi Xie and Andrew Zisserman. Multicolumn networks for face recognition. *arXiv preprint arXiv:1807.09192*, 2018.

[73] Jianwei Yang, Zhile Ren, Chuang Gan, Hongyuan Zhu, and Devi Parikh. Cross-channel communication networks. In *NeurIPS*, 2019.

[74] Dong Yi, Zhen Lei, Shengcai Liao, and Stan Z Li. Learning face representation from scratch. *arXiv:1411.7923*, 2014.

[75] Xi Yin and Xiaoming Liu. Multi-task convolutional neural network for pose-invariant face recognition. *IEEE Trans. Image Processing*, 27(2):964–975, 2017.

[76] Julio Zamora Esquivel, Adan Cruz Vargas, Paulo Lopez Meyer, and Omesh Tickoo. Adaptive convolutional kernels. In *ICCV Workshops*, 2019.

[77] Rich Zemel, Yu Wu, Kevin Swersky, Toni Pitassi, and Cynthia Dwork. Learning fair representations. In *ICML*, 2013.

[78] Xiaoning Zhang, Tiantian Wang, Jinqing Qi, Huchuan Lu, and Gang Wang. Progressive attention guided recurrent network for salient object detection. In *CVPR*, 2018.

[79] Yuanyuan Zhang, Dong Zhao, Jiande Sun, Guofeng Zou, and Wentao Li. Adaptive convolutional neural network and its application in face recognition. *Neural Processing Letters*, 2016.

[80] Zhifei Zhang, Yang Song, and Hairong Qi. Age progression/regression by conditional adversarial autoencoder. In *CVPR*, 2017.

[81] Jieyu Zhao, Tianlu Wang, Mark Yatskar, Vicente Ordonez, and Kai-Wei Chang. Men also like shopping: Reducing gender bias amplification using corpus-level constraints. In *EMNLP*, 2017.

Mitigating Face Recognition Bias via Group Adaptive Classifier
(Supplementary Material)

Sixue Gong   **Xiaoming Liu**   **Anil K. Jain**
Michigan State University, East Lansing MI 48824
{gongsixu, liuxm, jain}@msu.edu

In this supplementary material we include; (1) Section 1: the statistics of datasets used in the experimental section, (2) Section 2: Performance of the pre-trained gender and race/ethnicity classifiers to provide GAC with demographic information, (3) Section 3: Bias comparison between GAC and its ablation variants.

1 Datasets

Tab. 1 summarizes the datasets we adopt for conducting experiments, which reports the total number of face images and subjects (identities), and the types of demographic annotations. In the cross-validation experiment In Tab. 2, we report the statistics of each data fold for the cross-validation experiment on BUPT-Balancedface and RFW datasets.

Datasets	# of Images	# of Subjects	Demographic Annotations
IMDB [10]	460, 723	20, 284	Gender, Age
UTKFace [14]	24, 106	-	Gender, Age, Race/ethnicity
AgeDB [8]	16, 488	567	Gender, Age
AFAD [9]	165, 515	-	Gender, Age, Ethnicity (East Asian)
AAF [1]	13, 322	13, 322	Gender, Age
RFW [13]	665, 807	-	Race/Ethnicity
BUPT-Balancedface [12]	1, 251, 430	28, 000	Race/Ethnicity
IMFDB-CVIT [11]	34, 512	100	Gender, Age Groups, Ethnicity (South Asian)
MS-Celeb-1M [4]	5, 822, 653	85, 742	No Demographic Labels
PCSO [2]	1, 447, 607	5, 749	Gender, Age, Race/Ethnicity
LFW [5]	13, 233	5, 749	No Demographic Labels
IJB-A [6]	25, 813	500	Gender, Age, Skin Tone
IJB-C [7]	31, 334	3, 531	Gender, Age, Skin Tone

Table 1: Statistics of training and testing datasets for the experiments in the paper

Fold	White (#)		Black (#)		East Asian (#)		South Asian (#)	
	Subjects	Images	Subjects	Images	Subjects	Images	Subjects	Images
1	1, 991	68, 159	1, 999	67, 880	1, 898	67, 104	1, 996	57, 628
2	1, 991	67, 499	1, 999	65, 736	1, 898	66, 258	1, 996	57, 159
3	1, 991	66, 091	1, 999	65, 670	1, 898	67, 696	1, 996	56, 247
4	1, 991	66, 333	1, 999	67, 757	1, 898	65, 341	1, 996	57, 665
5	1, 994	68, 597	1, 999	67, 747	1, 898	68, 763	2, 000	56, 703

Table 2: Statistics of Dataset Folds in the Cross-validation Experiment

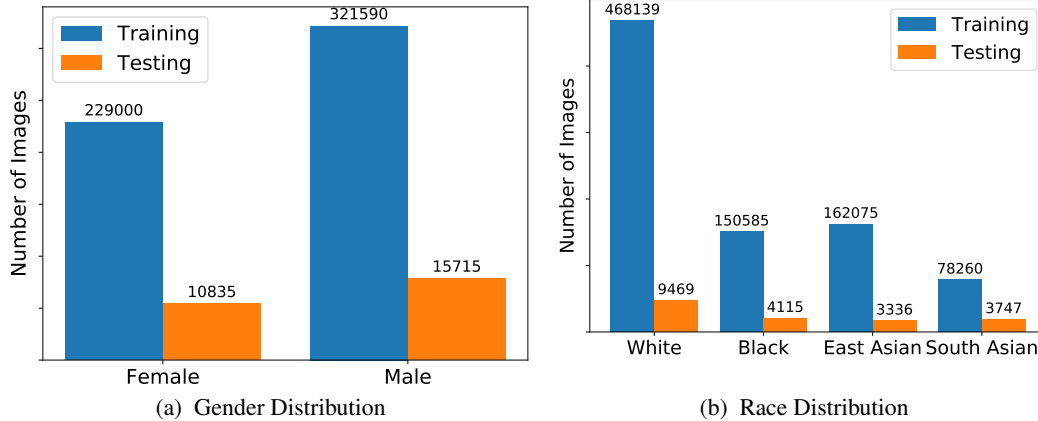(a) Gender Distribution   (b) Race Distribution

Figure 1: Statistics of the datasets for training and testing demographic attribute estimation networks. (a) The number of images in each gender group of the datasets for gender estimation; (b) The number of images in each race/ethnicity group of the datasets for race/ethnicity estimation.

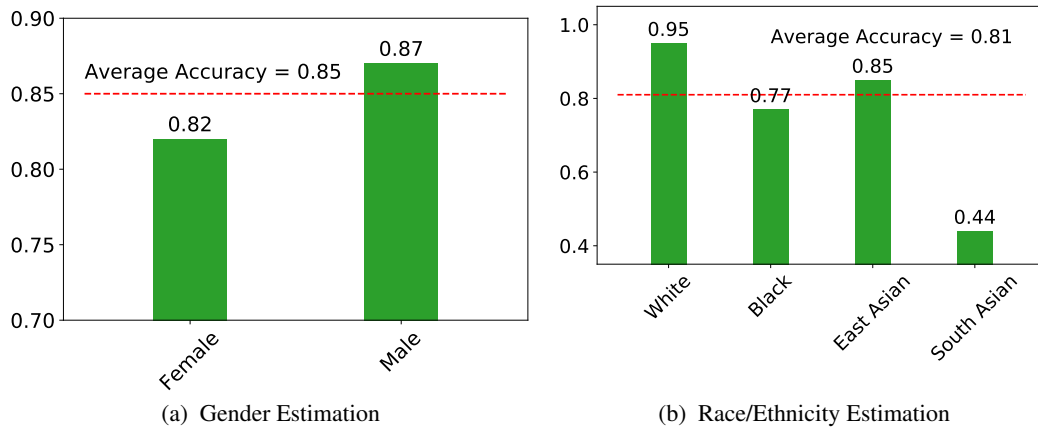(a) Gender Estimation   (b) Race/Ethnicity Estimation

Figure 2: Performance of the demographic attribute estimation networks. (a) The classification accuracy in each gender group; (b) The classification accuracy in each race/ethnicity group. The red dashed line shows the average performance.

2 Demographic Attribute Estimation

We train a gender classifier and a race/ethnicity classifier to provide GAC with demographic information during both training and testing procedures. We use the same datasets for training and evaluating the two demographic attribute classifiers as the work of [3]. The combination of IMDB, UTKface, AgeDB, AFAD, and AAF is used for gender estimation, and the collection of AFAD, RFW, IMFDB-CVIT, and PCSO is used for race/ethnicity estimation. Fig. 1 shows the total number of images in each demographic group of the training and testing set. Fig. 2 shows the performance of demographic attribute estimation on the testing set. For gender estimation, we see that the performance in the male group is better than that in the female group. For race/ethnicity estimation, the white group outperforms than the other race/ethnicity groups.

3 Bias Analysis

We extend Tab.4 in the main paper and compare the proposed GAC with other ablation variants. Tab. 3 reports the distribution parameters of the features extracted by different networks. By comparing the relative entropy (RE), we notice that GAC gives the smallest values in the three race/ethnicity groups than the other ablation methods, which shows the efficacy of GAC to mitigate the demographic bias.

2

Method	White			Black			East Asian			South Asian		
	Mean	STD	RE	Mean	STD	RE	Mean	STD	RE	Mean	STD	RE
Baseline	1.15	0.30	0.00	1.07	0.27	0.61	1.08	0.31	0.65	1.15	0.31	0.19
GAC-Channel	1.17	0.30	0.00	1.11	0.28	0.43	1.10	0.32	0.63	1.17	0.31	0.20
GAC-Kernel	1.18	0.29	0.00	1.09	0.28	0.42	1.10	0.31	0.59	1.17	0.31	0.19
GAC-Spatial	1.14	0.32	0.00	1.10	0.29	0.60	1.10	0.30	0.65	1.16	0.30	0.17
GAC-CS	1.16	0.31	0.00	1.09	0.28	0.46	1.09	0.32	0.62	1.17	0.31	0.18
GAC-CSK	1.17	0.31	0.00	1.11	0.28	0.51	1.10	0.32	0.63	1.18	0.31	0.18
GAC-($\tau = -0.1$)	1.17	0.31	0.00	1.11	0.28	0.43	1.10	0.32	0.61	1.17	0.30	0.20
GAC-($\tau = 0.1$)	1.16	0.31	0.00	1.10	0.27	0.45	1.10	0.32	0.62	1.18	0.32	0.17
GAC	1.17	0.31	0.00	1.10	0.28	0.43	1.10	0.32	0.58	1.18	0.32	0.13

Table 3: Distribution of ratios between minimum inter-class distance and maximum intra-class distance of face features in 4 race groups of RFW. GAC exhibits higher ratios, and more similar distributions to the reference.

References

[1] Jingchun Cheng, Yali Li, Jilong Wang, Le Yu, and Shengjin Wang. Exploiting effective facial patches for robust gender recognition. *Tsinghua Science and Technology*, 24(3):333–345, 2019.

[2] Debayan Deb, Lacey Best-Rowden, and Anil K Jain. Face recognition performance under aging. In *CVPRW*, 2017.

[3] Sixue Gong, Xiaoming Liu, and Anil K Jain. Debface: De-biasing face recognition. *arXiv preprint arXiv:1911.08080*, 2019.

[4] Yandong Guo, Lei Zhang, Yuxiao Hu, Xiaodong He, and Jianfeng Gao. Ms-celeb-1m: A dataset and benchmark for large-scale face recognition. In *ECCV*, 2016.

[5] Gary B Huang, Marwan Mattar, Tamara Berg, and Eric Learned-Miller. Labeled faces in the wild: A database forstudying face recognition in unconstrained environments. 2008.

[6] Brendan F Klare, Ben Klein, Emma Taborsky, Austin Blanton, Jordan Cheney, Kristen Allen, Patrick Grother, Alan Mah, and Anil K Jain. Pushing the frontiers of unconstrained face detection and recognition: Iarpa janus benchmark a. In *CVPR*, 2015.

[7] Brianna Maze, Jocelyn Adams, James A Duncan, Nathan Kalka, Tim Miller, Charles Otto, Anil K Jain, W Tyler Niggel, Janet Anderson, Jordan Cheney, et al. IARPA janus benchmark-c: Face dataset and protocol. In *2018 ICB*, 2018.

[8] Stylianos Moschoglou, Athanasios Papaioannou, Christos Sagonas, Jiankang Deng, Irene Kotsia, and Stefanos Zafeiriou. Agedb: the first manually collected, in-the-wild age database. In *CVPRW*, 2017.

[9] Zhenxing Niu, Mo Zhou, Le Wang, Xinbo Gao, and Gang Hua. Ordinal regression with multiple output cnn for age estimation. In *CVPR*, 2016.

[10] Rasmus Rothe, Radu Timofte, and Luc Van Gool. Deep expectation of real and apparent age from a single image without facial landmarks. *IJCV*, 2018.

[11] Parisa Beham Jyothi Gudavalli Menaka Kandasamy Radhesyam Vaddi Vidyagouri Hemadri J C Karure Raja Raju Rajan Vijay Kumar Shankar Setty, Moula Husain and C V Jawahar. Indian Movie Face Database: A Benchmark for Face Recognition Under Wide Variations. In *NCVPRIPG*, 2013.

[12] Mei Wang and Weihong Deng. Mitigate bias in face recognition using skewness-aware reinforcement learning. *arXiv preprint arXiv:1911.10692*, 2019.

[13] Mei Wang, Weihong Deng, Jiani Hu, Xunqiang Tao, and Yaohai Huang. Racial faces in the wild: Reducing racial bias by information maximization adaptation network. In *ICCV*, 2019.

[14] Zhifei Zhang, Yang Song, and Hairong Qi. Age progression/regression by conditional adversarial autoencoder. In *CVPR*, 2017.